

## FEDSM-ICNMM2010-30+, ' '

### PLATINUM SUPPORTED MESOPOROUS SILICA SPHERES BY OPTIMIZED MICROFLUIDIC SOL-GEL SYNTHESIS SCHEME

#### Venkatachalam Chokkalingam

Experimental Physics, Saarland University  
66123 Saarbrücken, Germany.  
Max Planck Institute for Dynamics and Self-Organization  
Bunsenstr. 10, 37073 Goettingen, Germany.  
venkat.chokkalingam@physik.uni-saarland.de

#### Boris Weidenhof

Technical Chemistry, Saarland University,  
66123 Saarbrücken, Germany.  
b.weidenhof@mx.uni-saarland.de

#### Wilhelm F. Maier

Technical Chemistry, Saarland University,  
66123 Saarbrücken, Germany.  
w.f.maier@mx.uni-saarland.de

#### Stephan Herminghaus

Max Planck Institute for Dynamics and Self-Organization  
Bunsenstr. 10, Goettingen 37073, Germany.  
stephan.herminghaus@ds.mpg.de

#### Ralf Seemann

Max Planck Institute for Dynamics and Self-Organisation, Bunsenstr. 10, Goettingen 37073, Germany.  
Experimental Physics, Saarland University, 66123 Saarbrücken, Germany  
ralf.seemann@ds.mpg.de

#### ABSTRACT

Droplet based microfluidics is used to perform sol-gel reactions. The chemicals are dispensed, mixed, and pre-processed inside a microfluidic device allowing for long operation times without any clogging. Using this approach and optimizing all reaction and processing parameters we generate mesoporous silica particles with a very high surface area of  $820 \text{ m}^2 \text{ g}^{-1}$  and a narrow pore radius distribution of around 2.4 nm. To take full advantage of the possibilities offered by this microfluidic synthesis route, we produced platinum supported silica microspheres (as high as 7 mol. %) for heterogeneous catalysis.

**Keywords:** emulsions, chemical reactions, silica particles, sol-gel, catalysis.

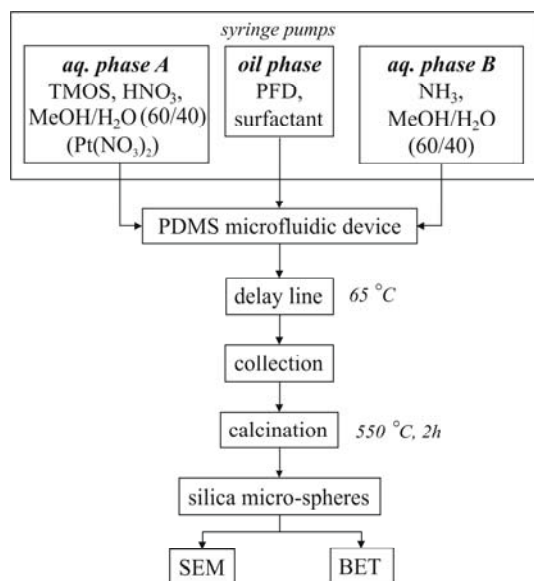
#### BACKGROUND AND MOTIVATION

In recent years, the interest in droplet based microfluidics increased due to the promising applications of this concept [1,2]. The droplets might act as micro-reactors containing well-defined quantities of reactants and overcome the limitations of single-phase microfluidic systems with their inherent capability of precise process control [3]. As a step towards droplet based synthesis, microfluidic devices have

been reported to produce microparticles within microfluidic devices. Polymeric particles can be produced quite easily by cross-linking monodisperse droplets e.g. from photo-curable pre-polymers [4,5]. For many applications like high performance liquid chromatography (HPLC) [6], drug delivery systems (DDS) [7,8] and versatile catalyst supports [9] it is furthermore desirable to produce mesoporous silica particles with large internal surface area and catalysts doped with metal-organic precursor solutions. But in contrast to organic polymers, the synthesis of silicate glasses by means of a sol-gel process is much more demanding. Droplets formed by a reactive sol-gel solution cannot be just cured instantaneously by e.g. UV or heat treatment. The sol-gel process with alkoxide-based systems usually comprise successive hydrolysis and condensation reactions to form a 3-D network followed by an aging step leading to the final porous glass [10]. The required volume controlled reactions and fast mixing can be achieved in droplet based microfluidics but poses a challenge for microfluidic approaches, where these requirements are circumvented by mixing the chemicals outside of the microfluidics device and injecting reactive solutions just to form droplets in the microfluidics device. This approach is quite simple but typically leads to fast clogging of the microfluidics device.

Recently, Carroll *et al.* [11], and Lee *et al.* [12] developed synthesis procedures for silica microspheres in microfluidic devices by emulsifying a water-based precursor solution in a continuous oil phase. In both approaches the content of the sol-gel solution is soluble in the continuous phase and the formation of mesoporous silica particles is supported by templating surfactant species. Carroll *et al.* [11] used a two step processes where the droplets are generated inside a microfluidic device and collected outside at elevated temperature and reduced pressure to allow for evaporation-induced self-assembly (EISA) [13]. In contrast, Lee *et al.* [12] incorporated the evaporation of the solvent into the microfluidic device. They increased the residence time and allowed for the diffusion of the solvent into the surrounding oil phase. As a result they achieve core/shell type mesoporous particles. Carroll *et al.* [11] estimated the internal surface area of their produced silica particles to about  $500 \text{ m}^2\text{g}^{-1}$  based on results from batch processing using the identical chemical route [14]. Chen *et al.* [15] used an approach similar to Carroll *et al.* but on a significantly larger scale. They determined the internal surface areas of the produced silica particles to  $550 - 675 \text{ m}^2\text{g}^{-1}$  and the total pore volume  $1.1 - 2.6 \text{ cm}^3\text{g}^{-1}$ , depending on experimental parameter. However, to date no microfluidic synthesis of mesoporous silica spheres with very high specific surface area has been demonstrated by explicitly measuring their internal surface area. This might be a result of the limited operation time of the microfluidics device due to clogging.

Here, we take full advantage of the possibilities offered by droplet based microfluidics. To perform complex sol-gel chemical reactions without clogging the microchannels we apply a microfluidic synthesis scheme that is sketched in scheme 1. Droplets of two different solutions are produced, merged, mixed, and pre-processed inside a microfluidic device. We demonstrate the power of this microfluidic approach producing silica particles with extremely large internal surface areas of about  $820 \text{ m}^2\text{g}^{-1}$  even without surfactant templating.



Scheme 1. Synthesis route.

## EXPERIMENTAL SECTION

Poly (dimethylsiloxane) soft lithographic techniques were used to fabricate microchannels with rectangular cross sections and sealed to glass cover slips using a plasma cleaner (Diener electronic GmbH, Germany). Droplets A contain an acidified solution of 1.5 M tetramethoxysilane (TMOS, ABCR GmbH & Co. KG) in a mixture of methanol (Merck KGaA, Darmstadt, Germany) and water (MilliporeTM water) (60/40 v/v). Droplets B contain ammonia (Merck KGaA, Darmstadt, Germany) based on the same solvent (methanol/water 60/40 v/v). The final molar ratio was  $\text{TMOS/methanol/HNO}_3/\text{NH}_3/\text{H}_2\text{O} = 1:17.767:0.129:0.333:34.265$ . For platinum supported silica particle production, we dispensed 3 mol. % and 5 mol. %  $\text{Pt}(\text{NO}_3)_2$  (ABCR GmbH, Germany) in the aqueous phase A. The continuous phase consists of perfluorodecalin (PFD;  $\text{C}_{10}\text{F}_{18}$ , ABCR GmbH & Co. KG), where none of the dispersed reactants is soluble. To stabilize the droplets 20 wt.% of perfluorinated surfactant (penta decafluoro-1-octanol,  $\text{C}_8\text{H}_3\text{F}_{15}\text{O}$ , ABCR GmbH & Co. KG) is added to the continuous phase.

Microchannels were rendered fluorophilic by flushing the microchannels with 40 wt.% of the selected surfactant for about one hour before starting the flow with appropriate liquids. Aqueous and fluorous liquids were dispensed from gastight syringes (Hamilton Bonaduz AG, Switzerland), which were connected to the microfluidic device by Teflon tubing (Novodirect GmbH, Germany). Syringes were driven by home built computer controlled syringe pumps for accurate adjustment of the flow rates. In all of our experiments we used constant volumetric flow rates. Microphotographs were acquired with a high speed CMOS camera system (PCO 1200 hs). Specific surface area and pores size analysis were obtained using a Carlo Erba Sorptomatic 1990. The produced silica particles (170 mg) were loaded and degassed at  $200 \text{ }^\circ\text{C}$  for 2 h in vacuum, followed by analysis at  $77 \text{ K}$  with  $\text{N}_2$  as the adsorbate gas. The specific surface area was determined using the BET (Brunauer, Emmett, and Teller) multipoint method. The pore distribution was calculated by the B.J.H. (Barrett-Joyner-Halenda) method. TGA-DSC was performed using a Thermo-Gravimetric Analyzer (TGA) (Mettler-Toledo GmbH, Germany). The instrument was calibrated with Indium, Zinc, Aluminium and Gold supplied by Mettler-Toledo. Sample powder (approx. 10 mg) was manually filled into alumina cup and heated at ramp rates of  $10 \text{ }^\circ\text{C}/\text{min}$  from ambient temperature to  $800^\circ\text{C}$ . The reference material was an empty alumina cup. A flow of synthetic air,  $40 \text{ ml}/\text{min}$ , was maintained during the experiment. Gases evolved during the measurement were monitored online with a Balzers ThermoStar GSD 300 T quadrupole mass spectrometer connected to the thermogravimetric analyzer by a heated quartz glass capillary. SEM images were recorded with a Hitachi S-4500 scanning electron microscope operating at  $10 \text{ kV}$ .

## RESULTS AND DISCUSSION

To achieve the sol-gel reaction inside microfluidic devices, two “families” of monodisperse droplets (aq. phase A and B) are pairwise emulsified in an oil phase

(perfluorodecalin, PFD) where none of the dispersed components is soluble. To improve the formation of the aqueous droplets and to stabilize them in the continuous PFD oil phase, an oil-soluble surfactant (penta decafluoro-1-octanol) is added. For the production of the droplet pairs a self-synchronizing double step-emulsification system is used [16,17] (Figure 1a and b). With this technique strictly alternating pairs of droplets containing the different chemicals can be produced at frequencies of up to about 500 Hz with excellent monodispersity of better than 1.2 % (variance of the droplet diameters measured right after generation). Here, the two production units synchronize themselves via a pressure cross talk caused by the formation of the droplets.

One type of droplets (A) consists of an acidified solution of the silica precursor TMOS ( $\text{Si}(\text{OCH}_3)_4$ ) in a mixture of methanol/water (volume fraction of methanol: 60%) and  $\text{Pt}(\text{NO}_3)_2$ . The rapid acid catalyzed hydrolysis of tetramethoxysilane occurs in the solution before dispensing it into droplets A (pH 1-2). Taking into account that the high molar ratio of  $\text{Si}:\text{H}_2\text{O}$  ( $r > 10$ ), present in droplet A, combined with the nearly nonexistent retarding effect of the methoxide group on the hydrolysis rate additionally promotes the reaction. A rapid and nearly quantitative hydrolysis of the precursor to silicic acid within a few minutes can be assumed [18]. The second type of droplets (B) contains ammonia solution based on the same solvent (mixture of methanol and water with volume fraction of methanol: 60%). In a second step, the sol-gel reaction, i.e. the condensation of silicic acid, is accelerated by increasing the pH above the isoelectric point of silica (pH > 3). This is done by combining and mixing one droplet A with one droplet B (ammonia solution) inside the microfluidic device whereas none of the liquids gets in contact with the microfluidic channels. By combining the two droplets the pH is adjusted to be between pH 6 and pH 7, where the gel time is minimal [19]. The first step of condensation is the deprotonation of silanols by reaction with hydroxyl ions. The condensation of deprotonated silanols combined with aggregation of the condensed species leads to a continual growth of the formed polymer up to a point where the silica particles become too large to be solvated. Apart from condensation, the dissolution of silica by means of alcoholysis and hydrolysis of siloxane bonds (reverse reactions of condensation) also exhibits a strong pH-dependency which increases by more than three orders of magnitude between pH 3 and 8 in aqueous solution [20]. Taking into account, that the content of methanol in the final droplet is much higher than that of water, a rather low dissolution rate can be assumed since the solubility of silica in methanol is much lower than in water. After a delay time at elevated temperature, the gelled droplets are collected outside the microfluidics device.

The individual pairs of droplets produced from aqueous phases A and B dispersed in the continuous oil phase PFD were coalesced by forcing them into a geometrical constriction [21] behind the emulsification unit (Figure 1b). The flow velocity of the first droplet arriving at the geometrical constriction is reduced and the second droplet is pushed towards the first. This small impulse is sufficient to destabilize the lamellae and to induce coalescence of the droplet pairs. To guarantee the perfect function of this kind of coalescence it is

mandatory that the droplets arrive as pairs separated by only a thin layer of continuous phase from the next droplet pair. This is achieved by slight differences in the respective volumes of the droplet A and B. The smaller droplet will flow faster and catches up with the bigger droplet after a short traveling distance. An emulsion that is too stable to be coalesced by a geometric constriction can alternatively be destabilized applying by an electric field between two consecutive droplets [22]. This technique also works well for droplets of equal volumes.

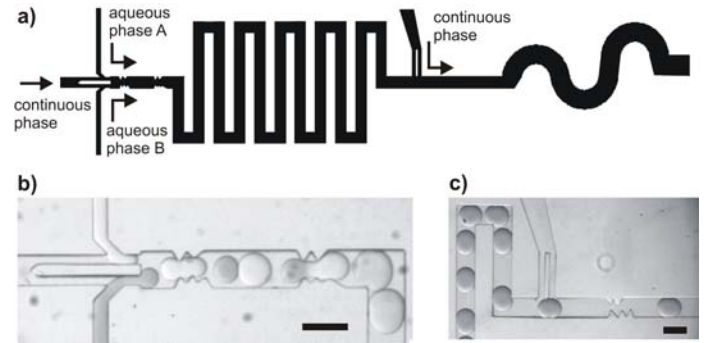


**Figure 1.** a) Schematic representation of the microfluidic device, b) Self-synchronized pairwise production of monodisperse droplets of different kind using a double step-emulsification device (channel depth 120  $\mu\text{m}$ ) with downstream merging of droplet pairs by a geometrical constriction. For clarity the aqueous phase injected from the bottom channel is colored with Nile blue. c) End of back fold channel geometry with side channel to inject continuous phase to increase the inter droplet distance. Scale bar: 200  $\mu\text{m}$ .

Downstream mixing of the reactants proceeds very efficiently due to the twisty flow pattern inside the droplets [3]. In the presented experiments mixing of the reactants within the droplet is performed within a travel distance of 500  $\mu\text{m}$ , which corresponds to about twice the drop length, respectively to about 100 ms at a typical flow velocity of about 8 mm/s. The mixing is very fast and completed within about 0.2 seconds depending on the flow velocity. The coalesced and mixed droplets (C) are subsequently given some time to develop the gel network in a delay line. To avoid the formation of clumps of silica gel at the rear side of the droplets [23], we reduce the motion induced flow pattern in the delay line by reducing the flow velocity. For that, the channel width is increased and guided into Teflon tubing with about ten times larger cross sectional area. To ensure that the droplets do not undergo any unwanted coalescences events in the delay line, the distance between coalesced droplets is further increased downstream by adding a small percentage of continuous oil phase after the serpentine channels and right before the delay line (Figure 1c). The Teflon tubing is coiled up in a temperature controlled chamber that is maintained at 65  $^{\circ}\text{C}$ . After a residence time of about 20 min in the Teflon tubing, the monodisperse silica-gel droplets (CV < 1.50 %, (Figure 2a)) are collected outside of the microfluidic device in a beaker containing the perfluorinated continuous phase, which is kept as well at 65  $^{\circ}\text{C}$ . In this beaker

the gel particles remain for another 2 h to ensure that the complete network formation has finished and to gently evaporate parts of the remaining solvent. Subsequently, the collected droplets (after evaporating the oil) are calcined and analyzed as will be described next. To determine the optimal calcination temperature for the synthesized silica gel spheres a thermo-gravimetric analysis was performed. The used analyzer was coupled with a mass spectrometer allowing an online examination of the exhaust gas. We found that, the PFD requires temperatures above 500 °C. Hence, all the collected droplets used for the analysis were calcined at 550 °C. The particles and their surface structure after calcinations are imaged by scanning electron microscopy SEM as shown in Figures 2b and 2c. The silica particles are almost perfectly round rarely showing small raised surface corrugations. The close-up of the particles shows a cloudy surface morphology, reminiscent of a crumble topping. The porosity and the pore volume of the synthesized silica particles are investigated by a BET (Brunauer, Emmett, and Teller) [24] analysis using nitrogen as adsorbate.

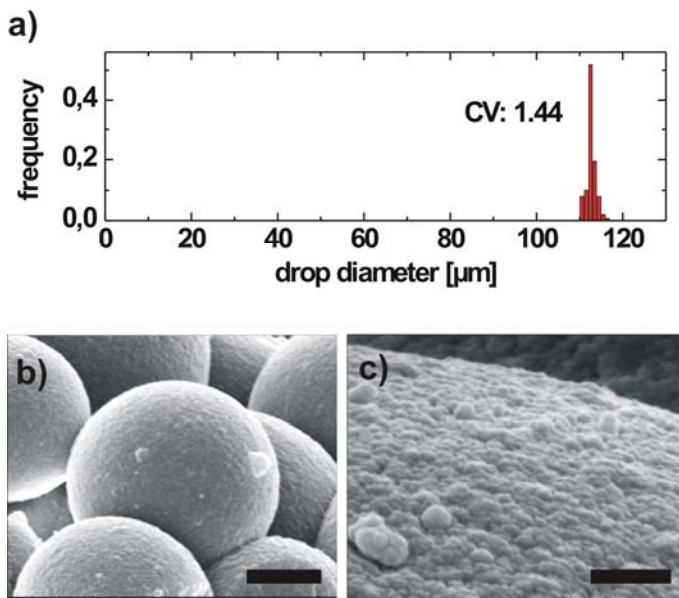


**Figure 2.** a) Histogram of the gel droplet sizes (before calcination) collected in the continuous phase outside the microfluidic device. Scanning electron micrographs of the silica spheres (after calcination): b) Silica spheres, scale bar: 1  $\mu\text{m}$ . c) Surface structure of silica spheres, scale bar: 100 nm.

A typical Nitrogen adsorption-desorption isotherm for the synthesized silica is shown in Figure 3. Various amounts of gas molecules will be adsorbed or desorbed at different doses of the gas. Knowing the area occupied by one adsorbate molecule,  $\sigma$  ( $= 16.2 \text{ \AA}^2$  for nitrogen), the total surface area of the material can be determined by the BET equation. The adsorption isotherm shows a steep rise in the low-pressure region at a normalized pressure of about  $p/p_0 < 0.05$  which could be interpreted as indication for the presence of micropores in the analyzed silica. However, the logarithmical

plot of the isotherm shows no inflexion point in this region, which signifies the absence of micropores in the sample [25].

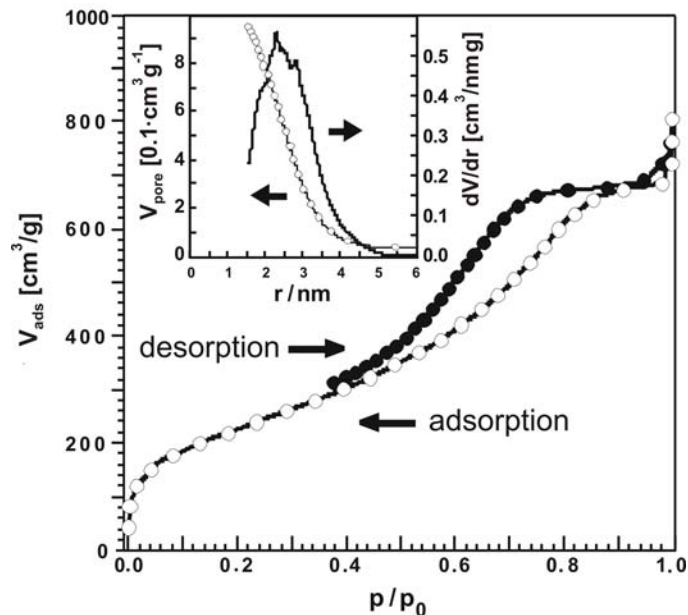


**Figure 3.** BET Nitrogen adsorption-desorption isotherm of silica spheres. Inset: pore size distribution from the desorption branch of the isotherm.  $V_{\text{ads}}$  = adsorbed volume,  $p/p_0$  = reduced pressure,  $V_{\text{pore}}$  = pore volume,  $r$  = pore radius.

At larger partial pressure a characteristic hysteresis loop appears, between a relative pressure of  $p/p_0 = 0.40$  and  $p/p_0 = 0.85$ . According to IUPAC [26,27] this type of isotherm can be classified as type IV and indicates the presence of mesopores (pore size 2-50 nm). Moreover, the shape of the hysteresis hints to cylindrical pores with bimodal pore openings [28]. The pore size distribution calculated from this adsorption isotherm is shown in the inset. The comparatively narrow pore size distribution (inserted plot in Figure 3) has a distribution maximum at 2.4 nm pore radius. The specific surface area of the produced silica particles averaged over several production runs and for various measurements results in  $820 \text{ m}^2\text{g}^{-1}$  ( $\pm 20 \text{ m}^2\text{g}^{-1}$ ) with a cumulative pore volume of  $0.93 \text{ cm}^3\text{g}^{-1}$  ( $\pm 0.02 \text{ cm}^3\text{g}^{-1}$ ). Note that the surface area of the spheres itself is just about  $1 \text{ m}^2\text{g}^{-1}$  which is negligible with respect to its internal surface area. Comparing these results with the specific surface area and the pore structure of silica prepared by sol-gel bulk synthesis under strong acidic- ( $\text{pH} < 2$ ) or strong basic conditions ( $\text{pH} > 12$ ) reveals significant differences. Both types of bulk synthesis usually lead to silica with specific surface areas in the range of 200 – 600  $\text{m}^2\text{g}^{-1}$ . Silica prepared under acidic conditions is normally microporous and exhibits a comparatively high surface area whereas the silica obtained under strong basic conditions (so called Stöber conditions<sup>[29]</sup>) has a low surface area and is nonporous (pseudo mesoporous) [30] The silica particles synthesized by our microfluidic approach are mesoporous as expected for a base catalyzed condensation at pH about 6 and consequently far away from the Stöber conditions. We extended this system by adding  $\text{Pt}(\text{NO}_3)_2$

to the aqueous phase A and were able to produce Pt supported on silica particles (Figure 4). The platinum content of these particles can be as high as 7 mol. % and the particles are expected to have a very large surface area. When compared to the surface structure of silica spheres in Figure 2b, it is clear that doping of Pt on silica ruptures the surface for 7 mol. %. This is currently studied in detail along with testing of these particles for catalytic activities using emissivity corrected Infra-Red Thermography (ecIRT) [31].

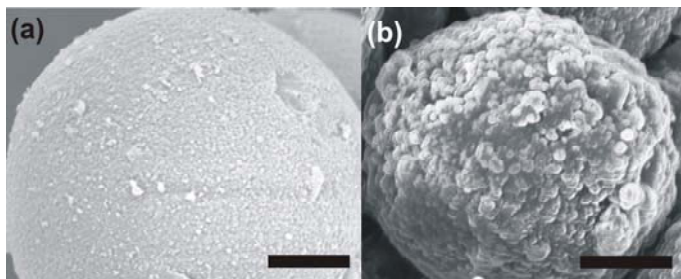


**Figure 4.** SEM images of Pt supported on silica microspheres. (a) 3 mol. %, (b) 7 mol. %. Scalebar: 1  $\mu\text{m}$ .

## CONCLUSION

In conclusion, we have presented droplet based microfluidics, to perform chemical synthesis by controlled merging and mixing of reactants inside droplets. The activation of chemical reactions inside droplets allows long operation times even for reactants that would otherwise clog microfluidic channels e.g. by sticking to the channel wall or precipitating. Furthermore, the well defined liquid volume and the fast mixing inside the droplets allow for precise stoichiometric synthesis even for fast chemical processes. We demonstrated this by producing monodisperse silica particles using combined acid-catalyzed hydrolysis and base-catalysed condensation for rapid gelation. All microfluidic processing steps were optimized to meet the particular requirements of mesoporous silica particle production. Using this approach we achieved mesoporous silica particles with a very high surface area of  $820 \text{ m}^2\text{g}^{-1}$  ( $\pm 20 \text{ m}^2\text{g}^{-1}$ ) and a narrow pore radius distribution of around 2.4 nm. Using the same microfluidic device, alternatively silica particles could be produced ranging from about  $1 \mu\text{m}$  to  $15 \mu\text{m}$  by adjusting the flow properties. By also varying the dimensions of the microfluidic device and the chemical concentrations we might easily extend the accessible range of particle sizes by more than one order of magnitude to both directions. The sol-gel process developed here for pure silica spheres can easily be modified to produce a large variety of mixed oxides [32]. Thus our results have also model character for a composition independent production of porous mixed oxide spheres, which cannot be produced by other methods capable of spherical silica production.

## ACKNOWLEDGMENTS

We thank the group of Prof. U. Hartmann for help with SEM measurements. This work was partially funded by the DFG project Se 1118/4.

## REFERENCES

- [1] Stone, Z. B.; Stone, H. A. *Physics of Fluids* 2005, 17, 063103-11.
- [2] F. Sarrazin, F. Sarrazin, K. Loubière, L. Prat, C. Gourdon, T. Bonometti, J. Magnaudet, *Aiche Journal* 2006, 52, 4061-4070.
- [3] H. Song, J. D. Tice, R. F. Ismagilov, *Angew. Chem., Int. Ed.* 2003, 42, 768-772.
- [4] M. Seo, Z. Nie, S. Xu, M. Mok, P. C. Lewis, R. Graham, E. Kumacheva, *Langmuir* 2005, 21, 11614-11622.
- [5] D. Dendukuri, K. Tsoi, T. A. Hatton, P. S. Doyle, *Langmuir* 2005, 21, 2113-2116.
- [6] L. C. Sander, S. A. Wise, *Analytical Chemistry* 2002, 67, 3284-3292.
- [7] R. F. H. Dekker, *Appl. Biochem. Biotechnol.* 1990, 23, 25-39.
- [8] Slowing, II, J. L. Vivero-Escoto, C. W. Wu, V. S. Y. Lin, *Advanced Drug Delivery Reviews* 2008, 60, 1278-1288.
- [9] D. E. De Vos, M. Dams, B. F. Sels, P. A. Jacobs, *Chemical Reviews* 2002, 102, 3615-3640.
- [10] C. J. Brinker, G. W. Scherer, *Sol-Gel Science: The Physics and Chemistry of Sol-Gel Processing*, Academic Press, Inc., Boston, 1990.
- [11] N. J. Carroll, S. B. Rathod, E. Derbins, S. Mendez, D. A. Weitz, D. N. Petsev, *Langmuir* 2008, 24, 658-661.
- [12] I. Lee, Y. Yoo, Z. Cheng, H.-K. Jeong, *Adv. Funct. Mater.* 2008, 18, 4014-4021.
- [13] C. J. Brinker, Y. Lu, A. Sellinger, H. Fan, *Adv. Mater.* 1999, 11, 579-585.
- [14] N. Andersson, B. Kronberg, R. Corkery, P. Alberius, *Langmuir* 2007, 23, 1459-1464.
- [15] Y. Chen, Y. J. Wang, L. M. Yang, G. S. Luo, *Aiche Journal* 2008, 54, 298-309.
- [16] V. Chokkalingam, S. Herminghaus, R. Seemann, *Appl. Phys. Lett.* 2008, 254101.
- [17] C. Priest, S. Herminghaus, R. Seemann, *Appl. Phys. Lett.* 2006, 024106.
- [18] J. C. Pouxviel, J. P. Boilot, J. C. Beloeil, J. Y. Lallemand, *Non-Cryst. Solids* 1987, 89, 345-360.
- [19] C. J. Brinker, G. W. Scherer, *Sol-Gel Science: The Physics and Chemistry of Sol-Gel Processing*, Academic Press, Inc., Boston, 1990.
- [20] R. K. Iler, *The Chemistry of Silica* Wiley, New York, 1979.
- [21] J. M. Kohler, et al, *Chem. Engg. Journal* 2004, 101, 201-216.
- [22] C. Priest, S. Herminghaus, R. Seemann, *Appl. Phys. Lett.* 2006, 134101; D.R. Link, E.G. Mongrain, A. Duri, F. Sarrazin, Z. Cheng, G. Cristobal, M. Marquez, and D.A. Weitz, 2006, *Angew. Chem. Int. Ed.*, 45, pp. 2556-2560.
- [23] H. M. Evans, E. Surenjav, C. Priest, S. Herminghaus, R. Seemann, T. Pföhl, *Lab on a Chip* 2009, 9, 1933-1941.

- [24] S. Brunauer, P. H. Emmett, E. Teller, *J. Am. Chem. Soc.* 1938, 60 (2), 309-319.
- [25] S. Storck, H. Bretinger, W. F. Maier, *Appl. Catal. A-Gen.* 1998, 174, 137-146.
- [26] K. S. W. Sing, *Pure Appl. Chem.* 1985, 57, 603-619.
- [27] S. Lowell, J. E. Shields, M. A. Thomas, M. Thommes, *Characterization of Porous Solids and Powders: Surface Area, Pore Size and Density*, Springer, Dordrecht, 2006.
- [28] J. C. P. Broekhoff, J. H. de Boer, *J. Catal.* 1968, 10, 368-376.
- [29] W. Stöber, A. Fink, E. Bohn, *J. Colloid Interf. Sci.* 1968, 26, 62-69.
- [30] I. C. Tilgner, P. Fischer, F. M. Bohnen, H. Rehage, W. F. Maier, *Microporous Mater.* 1995, 5, 77-90.
- [31] A. Holzwarth, W. F. Maier, *Platinum Metals Rev.*, 2000, 44, (1), 16-21.
- [32] G. Frenzer, W. F. Maier, *Annual Review of Materials Research* 2006, 36, 281-331.